Iranian Journal of Oil & Gas Science and Technology, Vol. 11 (2022), No. 1, pp. 70–81
http://ijogst.put.ac.ir

Defect Analysis in Functionally Graded Spherical Pressure Vessels

Hadi Eskandari[1*]

[1] Abadan Institute of Technology, Petroleum University of Technology, Abadan, Iran

Highlights

- 3D FEM evaluates SIFs in cracked functionally graded spherical vessels.
- Crack geometry governs critical fracture initiation zones.
- Material gradation strongly affects stress intensity factor distributions.
- Findings enhance fracture prediction in thermo-mechanically loaded SPVs.

Received: August 22 2020; *revised*: May 16, 2022; *accepted*: June 15, 2022

Abstract

This study investigates the stress intensity factor (SIF) in a cracked spherical pressure vessel. The vessel is assumed to be made of functionally graded material and contains a semi-elliptical surface crack. It is subjected to thermo-mechanical loading. Three-dimensional finite element analysis is performed to evaluate the SIFs along the crack front for a wide range of crack geometries and layer thicknesses. The elastic modulus of the sphere is assumed to vary exponentially in the radial direction of the vessel. The effect of a non-uniform coefficient of thermal expansion (CTE) on fracture parameters is also examined. The results show that the material gradation of the spherical pressure vessel significantly influences the distribution of SIFs along the crack front. Additionally, material gradation, wall thickness, and crack front profile affect the location of the critical point along the crack front, which is most susceptible to crack propagation.

Keywords: Crack analysis, Functionally graded material, Spherical pressure vessel.

How to cite this article
Eskandari, H., Defect Analysis in Functionally Graded, Spherical Pressure Vessels, Iran J. Oil Gas Sci. Technol., Vol. 11, No. 1, p. 70–81, 2022. DOI: https://doi.org/10.22050/ijogst.2022.244926.1560

1. Introduction

Spherical pressure vessels (SPVs) are widely used across various industries and are critical components in many engineering applications (Perl and Bernshtein, 2011, 2012). Alongside recent advancements in modern industries, the demand for functionally graded materials (FGMs) instead of conventional materials under extreme pressure and temperature conditions has increased (Afsar and Anisuzzaman, 2007). Ootao et al. (1999) optimized the material distribution in an FGM hollow sphere to achieve thermal stress relaxation.

Most recent studies in the literature have focused on cracked cylindrical vessels, while three-dimensional crack analysis in functionally graded SPVs has not been thoroughly addressed. Nami and Eskandari (2012) analyzed cracked FGM cylinders under various loading conditions. Moghaddam et al. (2013) studied hollow cylinders with graded materials and calculated mixed-mode stress intensity

* Corresponding author:
Email: eskandari@put.ac.ir

factors (SIFs). Habibi et al. (2020) investigated the effects of crack shape on SIFs in an FGM spherical pressure vessel.

In this study, we consider a pressurized functionally graded SPV containing an internal surface defect (Figure 1). The effects of variations in the thermal expansion coefficient and material properties on SIF distribution are analyzed. The ellipsoidal defect is characterized by two dimensionless parameters, $\xi = a/c$ and $\eta = a/t$, representing the aspect ratio and relative crack depth, respectively. Stress intensity factors along the crack front are calculated for different crack geometries.

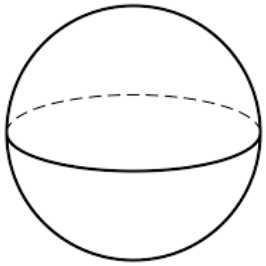

Figure 1

Spherical pressure vessels fixed at bottom region

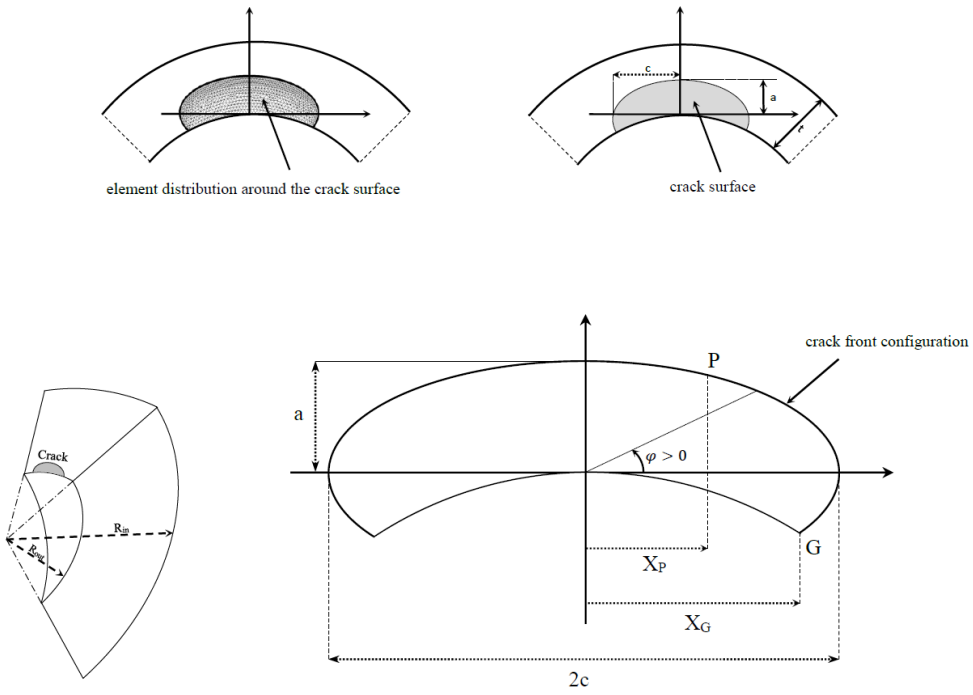

Figure 2

A functionally graded SPV containing a semi-elliptical surface defect

$$\gamma = \frac{1}{t}\ ln(\frac{\alpha_o}{\alpha_i}) \tag{1}$$

2. Finite element modeling (FEM)

This study aims to evaluate the stress intensity factors (SIFs) in a thermo-mechanically loaded functionally graded SPV. A sphere with an inner diameter of 20 mm and a wall thickness of 1 mm is considered. The sphere contains a semi-elliptical crack located on the internal surface of the vessel, as shown in Figure 2. Appropriate boundary conditions are essential to obtain accurate SIF values along the crack front. Internal pressure, P_{in}, is applied to the inner surface of the SPV at r=r_i, while the vessel is fixed ($u_x = u_y = u_y = 0$) over a small region on the outer surface opposite the crack.

Figure 2 illustrates the location of the semi-elliptical surface crack in the SPV. The x-coordinate of an arbitrary point P on the crack front, XP, is normalized by the corner point G coordinate, XG, i.e., $\psi = \frac{X_P}{X_G}$. The finite element model of the vessel is shown in Figure 3. Three-dimensional brick elements are employed, and the crack front is surrounded with singular elements to accurately capture the singular stress field at the crack tip.

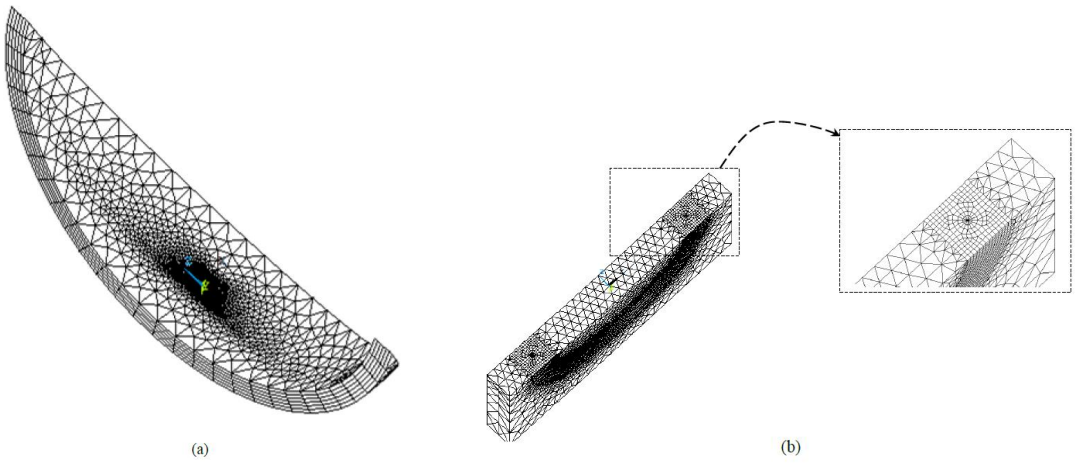

Figure 3

finite element model of a SPV containing inner crack: (a) the finite element model, (b) elements near the crack front

A finite element (FE) model using the ANSYS Parametric Design Language (APDL) is employed to evaluate the functional variation of material properties in the SPV. In this study, an isotropic material with exponential variation in Young's modulus and the thermal expansion coefficient through the SPV thickness is adopted, as follows:

$$E(r) = E_i\, e^{\phi\,(r-r_i)} \tag{2}$$

$$\alpha(r) = \alpha_i\, e^{\gamma\,(r-r_i)} \tag{3}$$

where r_i is the internal radius of the SPV, and ϕ and γ indicate the constants used for the description of the non-homogeneity in the material and thermal properties as defined below:

$$\phi = \frac{1}{\mathrm{t}} \ln\left(\frac{\mathrm{E_o}}{\mathrm{E_i}}\right) \tag{4}$$

$$\gamma = \frac{1}{t} \ln(\frac{\alpha_o}{\alpha_i}) \quad (5)$$

where *t* specifies the vessel thickness, and E_i, α_i and E_o, α_o denote the values of Young's modulus and the thermal expansions coefficient at the inner and outer radii of the SPV, respectively.

For example, an SPV with graded properties through the thickness is shown in Figure 4. For simplicity and traceability, a constant value of Poisson's ratio is used throughout the vessel.

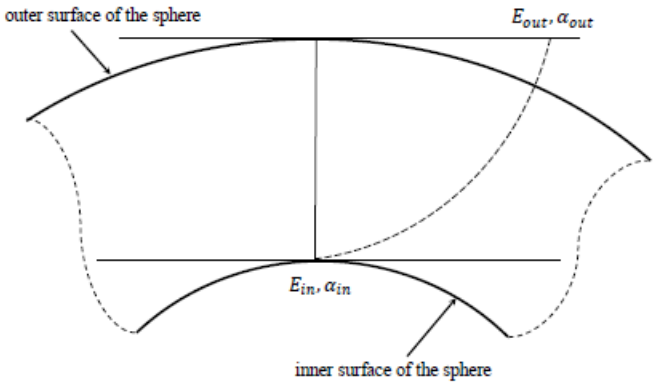

Figure 4

Spherical pressure vessel with functionally graded material through the thickness

The resulted dominant stress intensity factors, K_I, is normalized as follows:

$$K_{I,normalized} = \frac{K_I}{K_0} \quad (3)$$

Where the nominal SIF for the functionally graded SPV is calculated as follow:

$$K_0 = \frac{2\, P_{in}\, (r_o)^2}{(r_o)^2 - (r_i)^2} \sqrt{\frac{\pi a}{Q}} \quad \text{for plane stress} \quad (4)$$

where, the shape factor, *Q*, is suggested by Raju et al., (1980) as follows:

$$Q = 1 + 1.464\, (\frac{a}{c})^{1.65} \quad (5)$$

As is well known, nodes near the surface experience plane stress conditions, while the remaining nodes are subjected to plane strain conditions.

3. Stress intensity factor evaluation in FGMs

The non-homogeneous nature of FGMs has a significant influence on SIFs. Eischen (1987) established the stress fields around a crack tip in an FGM with spatially varying material properties, showing that, regardless of the functional variation in material properties, the nature of the stress

singularity is the same as in homogeneous materials. Therefore, the three modes of SIFs (K_I, K_{II}, K_{III}) can be determined using the crack opening displacement (COD) method (Zhang et al., 2011):

$$\begin{Bmatrix} K_{\mathrm{I}} \\ K_{\mathrm{II}} \\ K_{\mathrm{III}} \end{Bmatrix} = \frac{\mu_{\mathrm{tip}}\sqrt{2\pi}}{4(1-\nu)} \lim_{\delta \to 0} \frac{1}{\sqrt{\delta}} \begin{Bmatrix} \Delta u_{\xi}(\delta) \\ \Delta u_{\chi}(\delta) \\ (1-\nu)\Delta u_{\psi}(\delta) \end{Bmatrix} \tag{6}$$

where μ_{tip} is the shear modulus at the crack front. The distances from the crack front to a considered node on the crack surfaces in the local coordinate system are denoted as $\Delta u_{\varsigma,\chi,\psi}(\delta)$, where $\delta \longrightarrow 0$.

4. Numerical results

4.1. Validation of the method

A comprehensive review of the literature reveals a lack of reported results for functionally graded cracked SPVs in three-dimensional cases. Therefore, as shown in Figure 5a, we modeled a graded finite plate containing an elliptical crack under tensile stress loading using the FEM. As observed in Figure 5b, the results show good agreement for both homogeneous and graded plates with the findings reported by Yildirim et al. (2005).

4.2. Results and discussion

The resulting stress field in the studied case is shown in Figures 6a and 6b. As observed, stress concentration occurs near the crack front due to the singular elements employed around the crack tip.

In this study, a thermo-mechanically loaded spherical pressure vessel is investigated. The vessel is assumed to be made of FGM and subjected to an internal pressure of 5 MPa. The thermal gradient between the inner and outer surfaces of the vessel is assumed to be 45°C. A semi-elliptical defect is located on the inner surface of the vessel, as shown in Figure 2. The primary objective of this work is to examine the effects of material gradation in the SPV on SIF values along the crack front, thereby enabling analysis of fracture behavior. The problem is solved for various crack configurations, with a constant Poisson's ratio of 0.30 used throughout the material.

The variation of (K_I) along the crack front for an FGM and the corresponding homogeneous SPV is compared in Figures 7(a–e). Each curve is plotted for a constant (η = 0.2), a specific value of (ξ), and different material gradations ($RE = E_o/E_i$) of 0.2, 2, and 10. In these cases, the effect of thermal gradation is not considered.

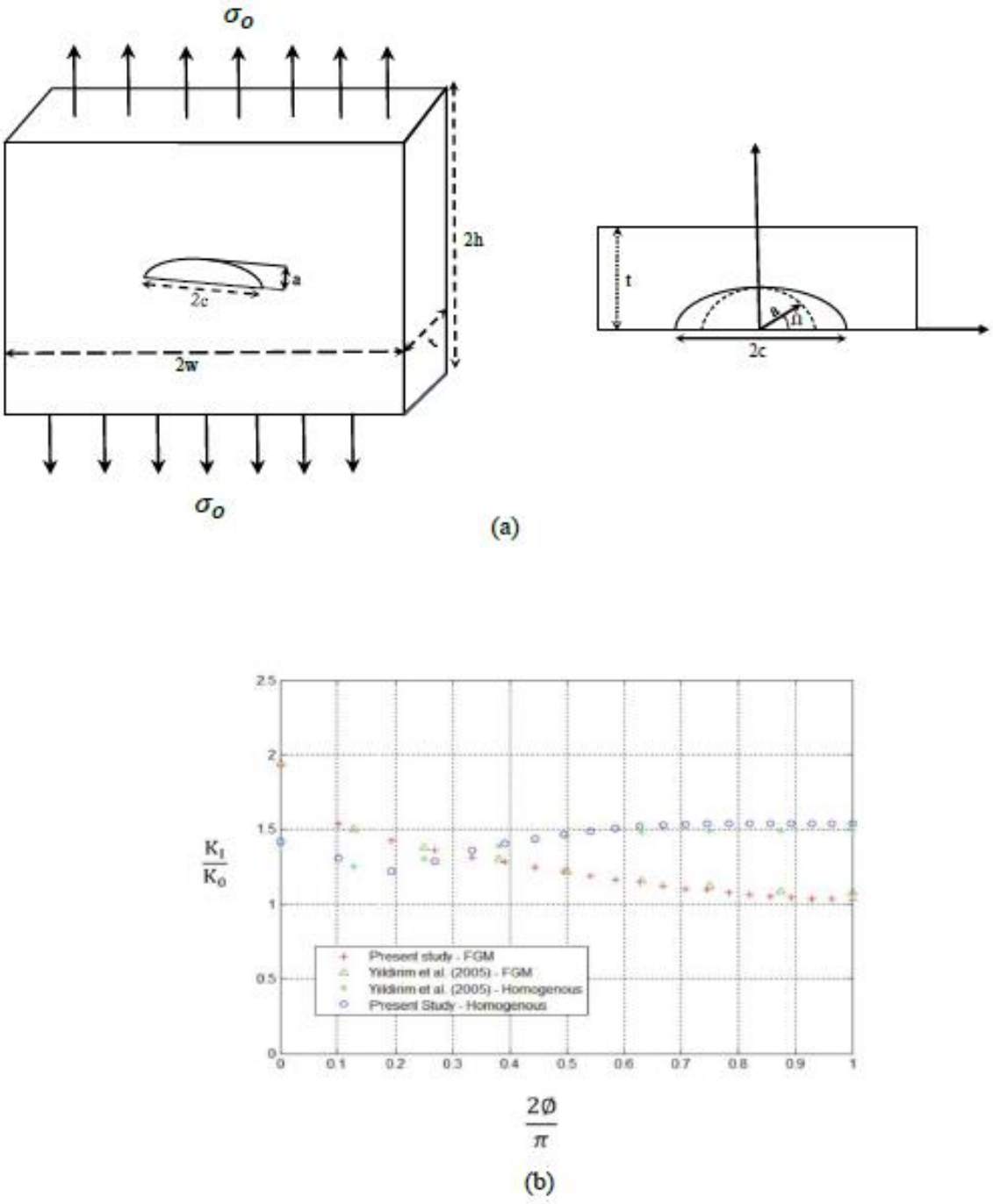

Figure 5

Semi-elliptical surface crack in an FGM plate under tension: a) schematic of the plate and crack configuration; b) distribution of the normalized (K_I) along the crack front for FGM and homogeneous plates with an aspect ratio of 1, relative crack depth of 0.8, , ν = 0.25 and $E(y{=}t)$ = 0.2.

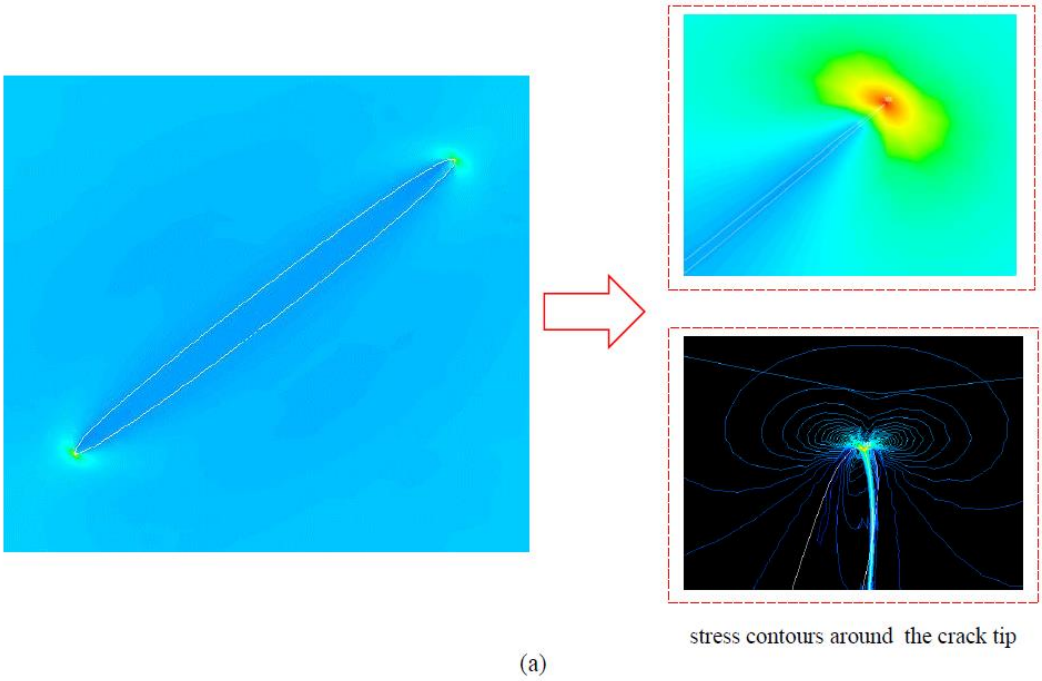

Figure 6

Finite element stress results around the crack: a) stress contours around the crack tip; b) stress intensity factors along the crack front.

It can be observed from Figure 7 that for $\frac{E_o}{E_i} \geq 1$, the value of K_I is directly dependent on RE. The variation of the SIF along the crack front in a graded SPV with RE ($\frac{E_o}{E_i} = 0.2$), a constant η, and different ξ values is illustrated in Figure 8. The following observations can be made:

- The K_I curve is symmetric with respect to the midpoint of the crack front, indicating that during crack growth, simultaneous propagation is expected at the corners.
- For $\frac{E_o}{E_i} \geq 1$, the SIF increases with increasing RE, which leads to a higher risk of crack propagation in SPVs.

- For a spherical pressure vessel made of graded material with low gradation ($\frac{E_o}{E_i} = 0.2$), the SIF near the deepest point of the crack front is higher than in a homogeneous vessel. In this case, the corners are safer than almost any other points.
- For large RE($\frac{E_o}{E_i} \gg 1$), points with zero parametric angle ($\phi = 0$) experience the minimum SIF. In other words, in SPVs with high gradation, the deepest points of the crack front are the most critical.

As shown in Figure 8, for an SPV with RE=2R and crack depth η=*a*/*t*=0.2, increasing ξ=*a*/*c* results in higher SIFs near the crack cusps ($\phi \rightarrow 0$). This indicates that for semicircular cracks ($\eta \rightarrow 1$), crack propagation along the surface is more likely than in the depth direction. This trend reverses for semi-elliptical cracks.

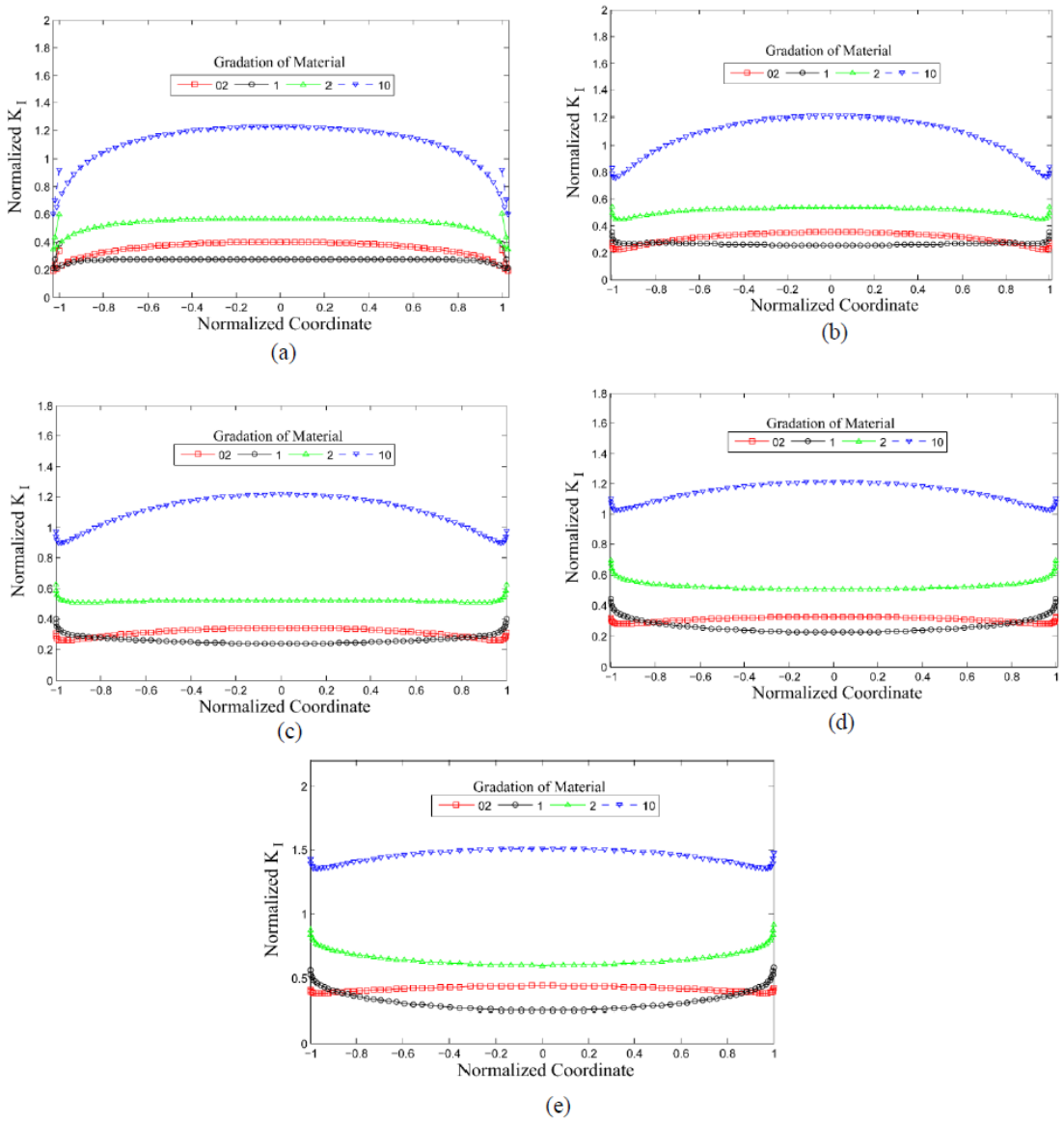

Figure 7

Distribution of K_I along the crack front in a graded SPV with t = 1 mm, η = 0.2, and α_2/α_1 = 1 for different values of aspect ratios (ξ); a) ξ = 0.2; b) ξ = 0.4; c) ξ = 0.6; d) ξ = 0.8; e) ξ = 1

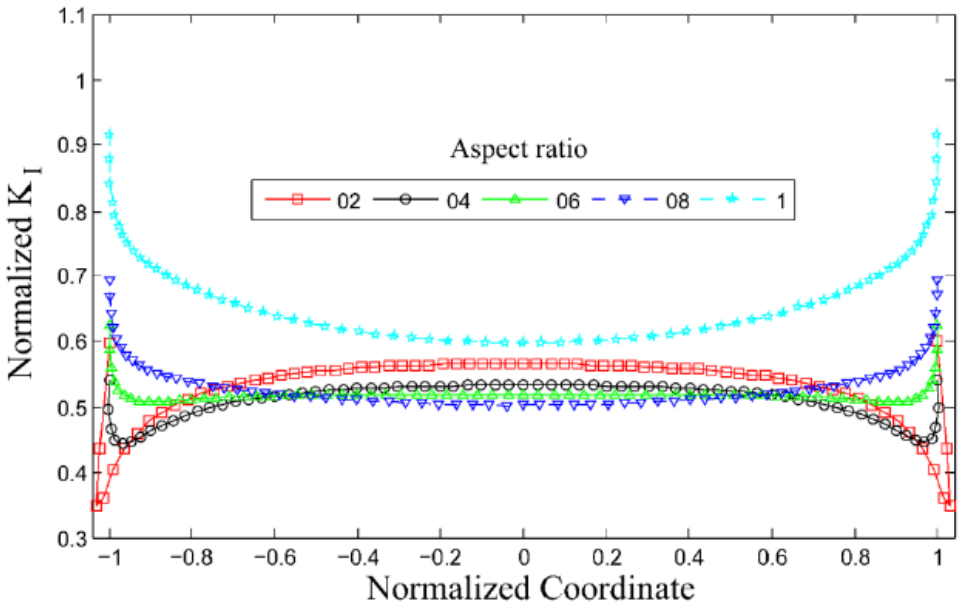

Figure 8

Variation of K_I through the crack line in a graded SPV (with RCTE=1, RE=2) for constant η = 0.2 and different aspect ratios: ξ = 0.2, 0.4, 0.6, 0.8, and 1.

The effects of thermal expansion gradation on K_I along the crack front (in the absence of material gradation) are shown in Figure 9. As observed, the SIF values are influenced by the thermal expansion gradation. For the same crack profiles, the SIFs in SPVs with thermal expansion gradation are generally higher than those in vessels graded only in mechanical properties.

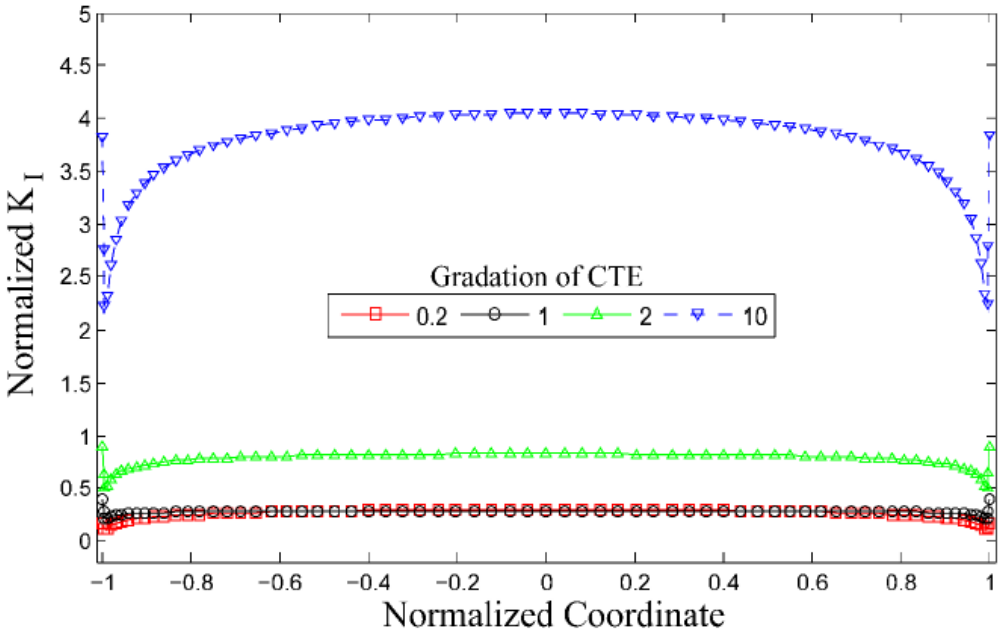

Figure 9

Distribution of the first mode stress intensity factor along the crack front in an exponentially varying thermal expansion FGM spherical pressure vessel with $\xi = \eta$ = 0.2 and different values of RCTE = α_2/α_1

The effects of wall thickness on SIF values are shown in Figures 10 and 11. A general analysis of the graphs reveals the following:

- In thick-walled functionally graded SPVs, smaller material gradation results in safer vessels regarding potential crack growth. For vessels with high material gradation (RE≫1), the maximum SIF occurs at the midpoint of the crack front.
- In thick-walled FGM spherical vessels, K_I increases with increasing wall thickness. In other words, points with zero parametric angles (ϕ=0) are more critical for crack propagation, while the corner points become the most vulnerable.
- The parametric angle (ϕ) at the crack cusps decreases as the wall thickness increases.

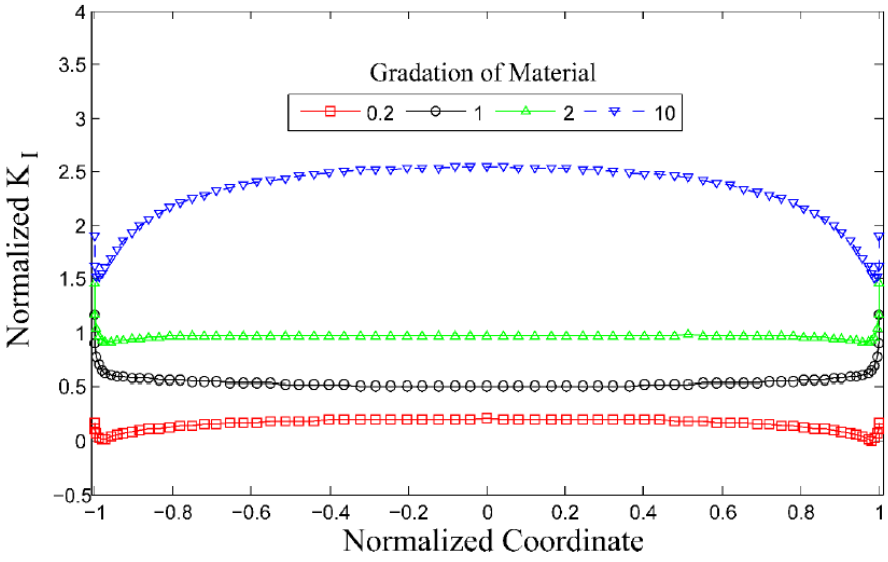

Figure 10

Distribution of K_I along the crack front in a functionally graded SPV with thickness of 2 mm, η = 0.2, α_2/α_1 = 1 for different values of RE

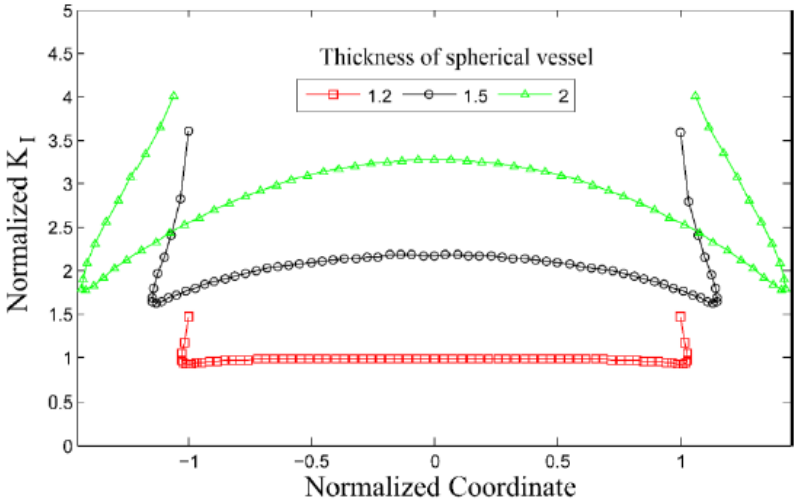

Figure 11

Distribution of K_I along the crack front in a functionally graded SPV with ξ = η = 0.4, α_2/α_1 = 1, RE = 2, and for different values of wall thickness

5. Conclusions

In this work, three-dimensional finite element analyses of a graded, pressurized spherical vessel with an embedded surface defect under thermo-mechanical loading are carried out. The effects of gradation in material properties and thermal expansion coefficients on SIF values along the crack front for different crack profiles are investigated. The results show that both material gradation and thermal expansion gradation can significantly influence the distribution and magnitude of SIFs along the crack front. Furthermore, material gradation, wall thickness, and crack profile can alter the locations of critical points for crack growth.

Acknowledgments

The authors acknowledge the technical support provided by the Research Center of Petroleum University of Technology, Abadan, Iran.

Nomenclatures

$a(mm)$	Depth of the deepest point on the crack front
APDL	ANSYS parametric design language
$c(mm)$	Semi axis of the elliptical crack
COD	Crack opening displacements
CTE	Coefficient of thermal expansion
$E(Pa)$	Elastic modulus
FEM	Finite element modeling
FGM	Functionally graded material
$K_I\ (Pa\sqrt{m})$	Conventional modes I stress intensity factor
$K_{i,non}$	Nondimensional modes I stress intensity factor
$K_O(Pa\sqrt{m})$	Nominal stress intensity factor
LNG	Liquefied natural gas
$P_{in}\ (Pa)$	Inner pressure of the vessel
Q	Shape factor
RCTE	Non-homogeneity ratio of the coefficient of thermal expansion
RE	Ratio of material non-homogeneity
$r_i(mm)$	Inner radius of the vessel
$r_o(mm)$	outer radius of the vessel
SIF	Stress intensity factor
$t(mm)$	Thickness of the vessel
TBC	Thermal barrier coating
$X_G\ (mm)$	x-coordinate of corner point on the crack front
$X_P\ (mm)$	x-coordinate of an arbitrary point on the crack front
$\Delta u(mm)$	Crack tip opening displacement
$\gamma(1/mm)$	Constant of thermal non-homogeneity
$\varepsilon(mm)$	Small distance near the crack tip
$\eta(mm/mm)$	Relative depth of the crack
$\mu(Pa)$	Shear modulus

$\xi(mm/mm)$	Aspect ratio
υ	Poisson's ratio
ϕ $(1/mm)$	Constant of material non-homogeneity
$\varphi(rad)$	Parametric angle
$\psi(mm/mm)$	Nondimensional normalized coordinates

References

Afsar, A.M., and Anisuzzaman, M., Stress intensity factors of two diametrically opposed edge cracks in a thick-walled functionally graded material cylinder. Eng. Fract. Mech. Vol. 74, p. 1617–1636 , 2007.

Eischen, J.W., Fracture of non-homogeneous materials. Int. J. Fract. Vol. 34, p. 3–22 . 1987.

Habibim, N., and Bahrampour, H, Estimation of the SIF in FGM spherical pressure vessel. Australian j. Mech. Eng. p. 1–24, 2020.

Moghaddam, A.S., Alfano, M., and Ghajar, R., Determining the mixed mode stress intensity factors of surface cracks in functionally graded hollow cylinders. Mater. Des. Vol. 43, p. 475–484, 2013.

Nami, M.R., and Eskandari, H., Three-dimensional investigations of stress intensity factors in a thermo-mechanically loaded cracked FGM hollow cylinder. Int. J. Pres. Ves. Pip. Vol. 89, p. 222–229, 2012.

Ootao, Y., Kawamura, R., Tanigawa, Y., and Imamura, R., Optimization of material composition of nonhomogeneous hollow sphere for thermal stress relaxation making use of neural network. Comput. Meth. Appl. Mech. Engng. Vol. 180, p. 185–201, 1999.

Perl, M., and Bernshtein, V., 3-D stress intensity factors for arrays of inner radial lunular or crescentic cracks in thin and thick spherical pressure vessels. Eng. Fract. Mech. Vol. 78, p. 1466–1477, 2011.

Perl, M., and Bernshtein, V., Three-dimensional stress intensity factors for ring cracks and arrays of coplanar cracks emanating from the inner surface of a spherical pressure vessel. Eng. Fract. Mech. Vol. 94, p. 71–84 , 2012.

Raju, I.S., and Newmann, Jr. JC. stress intensity factors for internal surface cracks in cylindrical pressure vessel. ASME J.P Press. Ves. Tech., Vol. 102, p. 342–356, 1980.

Yildirim, B., Dag, S., and Erdogan, F., Three-dimensional fracture analysis of FGM coatings under thermomechanical loading. Int. J. Fract. Vol. 132, p. 369–395 , 2005.

Zhang, C., Cui, M., Wang, J., Gao, X.W., Sladek, J., and Sladek, V., 3D crack analysis in functionally graded materials. Eng. Fract. Mech. Vol. 78, p. 585–604, 2011.

COPYRIGHTS
©2023 by the authors. Licensee Iranian Journal of Oil & Gas Science and Technology. This article is an open access article distributed under the terms and conditions of the Creative Commons Attribution 4.0 International (CC BY 4.0) (https://creativecommons.org/licenses/by/4.0/)